Journal of Physics: Condensed Matter

PAPER • **OPEN ACCESS**

How adsorbates alter the metallic behavior of quasi-1D electron systems of the Si(5 5 3)-Au surface

To cite this article: Michael Tzschoppe *et al* 2019 *J. Phys.: Condens. Matter* **31** 195001

OPEN ACCESS
IOP Publishing
Journal of Physics: Condensed Matter
J. Phys.: Condens. Matter **31** (2019) 195001 (9pp)
https://doi.org/10.1088/1361-648X/ab0710

How adsorbates alter the metallic behavior of quasi-1D electron systems of the Si(5 5 3)-Au surface

Michael Tzschoppe[1], Christian Huck[1,2], Fabian Hötzel[1], Benjamin Günther[3], Zamin Mamiyev[4], Andrey Butkevich[1], Constantin Ulrich[1], Lutz H Gade[3] and Annemarie Pucci[1,2]

[1] Kirchhoff Institute for Physics, Heidelberg University, Heidelberg, Germany
[2] Centre for Advanced Materials, Heidelberg University, Heidelberg, Germany
[3] Institute of Inorganic Chemistry, Heidelberg University, Heidelberg, Germany
[4] Institut für Festkörperphysik, Leibniz Universität Hannover, Hannover, Germany

E-mail: pucci@kip.uni-heidelberg.de

Received 5 October 2018, revised 1 February 2019
Accepted for publication 14 February 2019
Published 11 March 2019

Abstract

The plasmonic signals of quasi-1D electron systems are a clear and direct measure of their metallic behavior. Due to the finite size of such systems in reality, plasmonic signals from a gold-induced superstructure on Si(5 5 3) can be studied with infrared spectroscopy. The infrared spectroscopic features have turned out to be extremely sensitive to adsorbates. Even without geometrical changes of the surface superstructure, the effects of doping, of the adsorbate induced electronic surface scattering, and of the electronic polarizability changes on top of the substrate surface give rise to measurable changes of the plasmonic signal. Especially strong changes of the plasmonic signal have been observed for gold, oxygen, and hydrogen exposure. The plasmonic resonance gradually disappears under these exposures, indicating the transion to an insulating behavior, which is in accordance with published results obtained from other experimental methods. For C_{70} and, as shown here for the first time, TAPP-Br, the plasmonic signal almost retains its original intensity even up to coverages of many monolayers. For C_{70}, the changes of the spectral shape, e.g. of electronic damping and of the resonance position, were also found to be marginal. On the other hand, TAPP-Br adsorption shifts the plasmonic resonance to higher frequencies and strongly increases the electronic damping. Given the dispersion relation for plasmonic resonances of 1D electron systems, the findings for TAPP-Br indicate a push-back effect and therefore stronger confinement of the free charge carriers in the quasi-one-dimensonal channel due to the coverage by the flat TAPP-Br molecules. On the gold-doped Si(5 5 3)-Au surface TAPP-Br acts as counter dopant and increases the plasmonic signal.

Keywords: quasi-1D electron systems, infrared spectra, adsorbate induced effects

(Some figures may appear in colour only in the online journal)

1. Introduction

Metal-atom induced superstructures on Si [1–5] and Ge surfaces [6–8] have been studied intensely for more than two decades. It has been found that the atomic chains of these superstructures represent low-dimensional electron systems [2] which possess many surprising properties, such as metal-insulator transitions [9, 10] and spin ordering [11, 12]. The Si(5 5 3)-Au surface is a typical case of a quasi-1D system. A well-ordered surface is formed at a gold coverage of 0.48 monolayers (ML) [13]. This superstructure consists of 1.48 nm wide Si(1 1 1) terraces that are separated by monatomic steps [14, 15]. Density functional theory (DFT) modeling [11, 16], x-ray diffraction experiments [15], scanning tunneling microscopy (STM) [17], and spot-profile analysis low-energy electron diffraction (SPA-LEED) [18] have established a geometric structure consisting of a double Au chain running parallel to the step edges in the middle of the terrace and a chain of Si honeycombs at the step edge (see figure 1(a)). Electron-energy loss spectroscopy (EELS) also supports the 1D character of the electronic surface system [19]. With EELS the plasmonic dispersion relation has been measured [19], and the close corresponance of such a dispersion relation with the electronic bandstructure has been demonstrated recently [20]. Combined DFT and EELS studies have resolved a modest alteration of the electronic surface structure upon oxygen uptake for Au wires on Si(5 5 7) [21]. As studied by electron diffraction and four-tip STM-based transport experiments supported by DFT calculations, the Au–Si(5 5 3) surface also turned out to display almost inert behavior for O_2 exposures of up to at least 30 Langmuir (L) [22]. Adsorbate induced changes of the Si(5 5 3)-Au also have been investigated by a combination of reflectance anisotropy spectroscopy (RAS) and DFT [23]. Experimental and calculated RAS changes with hydrogen exposure have been interpreted as corresponding to a two-step process, starting from hydrogen adsorption at the step edges accompanied by a doping of originally metallic system and thus rendering it insulating. As second step, a recovery of the metallic property upon further hydrogen adsorption is predicted based on theoretical modeling though without experimental proof to date [23]. The step edges are especially chemically active and H bonding to Si at these step edges renders the system insulating [24]. Spin ordering at lower temperature has been theoretically predicted [10], and tiny changes of physical properties with decreasing temperature have been observed [11]. Hötzel *et al* have attributed this behavior to fluctuations of the electronic dipoles of the dangling bonds which are supressed by hydrogen adsorption [25]. With and without hydrogen adsorption the infrared resonance of plasmonic excitations of metallic chains (with finite length) shifts to different directions in frequency upon cooling. These tiny shifts of the order of 10 meV are clearly observed by infrared (IR) spectroscopy [25]. The high energy resolution has enabled new insights into the various consequences of adsorbates for the low-dimensional electronic system [26, 27]. In this work we compare the changes of the IR plasmonic resonance for the different adsorbate species, for H_2 and O_2 exposure and for deposition of Au, C_{70}, and TAPP-Br (a core brominated tetraazaperopyrene (TAPP) derivative with potential applications in organic electronics). By comparing the plasmonic resonance to a well established model, both the strength of the signal as a measure of the free-charge carrier density and information on the nature of the damping and confinement could be extracted.

2. Theoretical background

Plasmonic excitations can be observed by IR spectroscopy due to finite length of the plasmonic channels of the Si(5 5 3)-Au surface [28]. This results in standing waves of coherently oscillating electrons corresponding to oscillating electric dipoles (for the odd orders). The first order plasmonic mode gives a strong IR signal as in the case of bulky nanorods [29]. The IR resonance positions follow from the 1D plasmonic dispersion relation $\omega_{\mathrm{pl}}(q)$ that can be approximated for energies as low as in the middle IR by the relation

$$\omega_{\mathrm{pl}}(q) \approx (eq/n_{\mathrm{host}})\sqrt{n_{1\mathrm{D}}\ln(1/bq)/(2\varepsilon_0 m^*)} \qquad (1)$$

with q as the length of the wave vector, m^* as the effective mass of the electrons, $n_{1\mathrm{D}}$ as the 1D electron density, e as the elementary charge, and ε_0 as the vacuum permittivity. Equation (1) is derived from the theory of 1D electron systems [30–32] and considers the effect of the substrate and possible cover layers in terms of the refractive index n_{host} of a host. The confinement of the electron wave functions in the directions perpendicular to the chains is described by a Gaussian with width b. For finite wires of length l and assuming rigid ends, the standing wave vector of the fundamental mode can be estimated as $q = \pi/l$. Hence, the IR resonance position follows the proportionality

$$\omega_{\mathrm{pl}}(l) \propto \sqrt{n_{1\mathrm{D}}\ln(l/b\pi)/m^*}/(l\cdot n_{\mathrm{host}}). \qquad (2)$$

The absorption spectrum around that resonance position can be estimated as the classical absorption cross section σ_{abs} of a needle-like object with Drude-type metallic behavior [33, 34], which leads to

$$\sigma_{\mathrm{abs}} = \frac{n_{1\mathrm{D}} l e^2}{m^* \varepsilon_0 n_{\mathrm{host}} c} \frac{\omega^2 \omega_\tau}{\left[\left(\omega_{\mathrm{pl}}^2 - \omega^2\right)^2 + \omega^2\omega_\tau^2\right]}. \qquad (3)$$

In this relation ω is the circular photon frequency, ω_τ the electronic scattering rate, and c the vacuum velocity of light. By inserting the absorption cross section into the expression for the transmission of a very thin layer at normal incidence of light [35] the relative IR transmittance (normalized to the transmittance of the non-absorbing substrate with refractive index n_s) becomes

$$\frac{T_{\mathrm{Si+Au}}}{T_{\mathrm{Si}}} \approx 1 - \frac{2W}{(1+n_s)\sqrt{2\pi}\Delta\omega} \times \int_{-\infty}^{\infty} \exp\left\{-\frac{(x-\omega_{\mathrm{pl}})^2}{2\Delta\omega^2}\right\} \frac{\omega^2\omega_\tau}{\left[(x^2-\omega^2)^2+\omega^2\omega_\tau^2\right]}\mathrm{d}x \qquad (4)$$

with

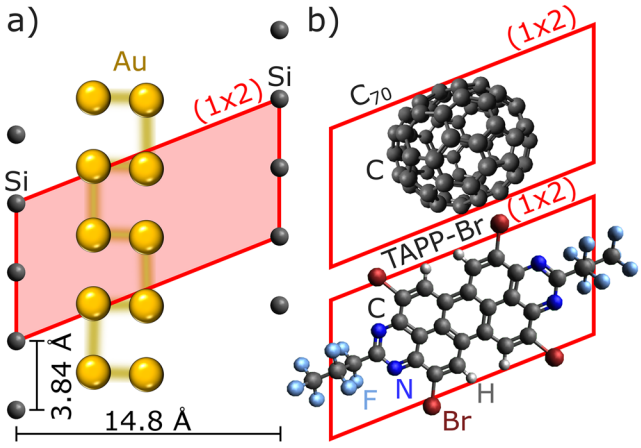

Figure 1. Surface structure model according to Hafke *et al* [18] with the 1×2 unit cell indicated. Only the Si atoms on the surface step edges are shown (a). A C_{70} molecule and a TAPP-Br-molecule, respectively, are shown with the same size scale as done in [27] to motivate our monolayer definition (b).

$$W = \frac{N}{A}\,\frac{n_{1D}\,l\,e^2}{\varepsilon_0 m^* c},$$

where $n_{1D}l$ is the number of oscillating electrons in one needle (conductive chain with length l on average). The factor N/A describes the number of wires N per surface area A. In equation (4), a Gaussian distribution [25–27, 36] of resonance frequencies with width $\Delta\omega$ is assumed because of the random distribution of wire lengths. Equation (4) is used as model function for the spectral fits for which each sample preparation might result in a different N/A but similar electronic properties of the conductive channels. Upon the adsorption of molecules, changes of the electronic scattering rate are to be expected because of the adsorbate induced surface resistivity [37–42] as well as the changes in n_{1D}/m^* due to charge transfer [26, 40]. In IR reflection-absorption spectroscopy of metal surfaces the adsorbate induced surface resistance is seen as a lowering of the broadband reflectance [38–42]. In IR transmittance spectra of ultrathin metal layers surface resistivity changes and charge transfer by adsorbates show up as broadband changes with different frequency dependent contributions [37]. As it will be seen in this work, the spectral changes of plasmonic resonances due to both the adsorbate-induced effects are different to those of non-resonant metallic surfaces.

The quantity n_{1D}/m^* may be considered as 1D analogue to the squared plasma-frequency parameter $\omega_p^2 \propto n_{3D}/m^*$ of the 3D Drude model (with n_{3D} as the free-charge carrier density in the 3D metal). We performed spectral fits to the measured IR spectra in which the fit parameters W, ω_τ, and the average ω_{pl} depend on the adsorbate coverage, but the parameter $\Delta\omega$ is kept fixed for each of the adsorption experiments.

3. Experimental methods and materials

3.1. Sample preparation and surface superstructure

The silicon surface was prepared in the same ultrahigh-vacuum (UHV) chamber and under the same procedures as reported in [25] at a base pressure below 10^{-10} mbar. For preparation, the Si(5 5 3) wafers (p-type doped, double side polished, 5–6 Ω cm resistivity, offcut angle of 12.3° from the [1 1 1] to [1 1 $\bar{2}$] direction) were heated at 600 °C for several hours and subsequently flash-annealed several times at temperatures up to 1250 °C in order to remove the native oxide layer and to prepare the vicinal Si(5 5 3) structure. The quality of the surfaces was checked by reflective high energy electron diffraction (RHEED), carried out with an acceleration voltage of 20 kV and an angle of incidence of around 1.5°. For the formation of the quasi-1D gold superstructures, 0.46 monolayers of Au ($1\ ML_{Au} \triangleq 7.83 \cdot 10^{14}$ Au atoms/cm^2) were evaporated onto the flashed silicon wafer which was held at room temperature (RT) as previously reported in [27]. For Au evaporation, a pyrolytic BN crucible and a deposition rate of 0.10 ML min^{-1} was chosen, with the total pressure never exceeding $3 \cdot 10^{-10}$ mbar during the course of the process. Evaporation rates for all experiments that we discuss in this paper were carefully checked and adjusted by using a quartz crystal microbalance. Additionally, low deposition rates were chosen to evaporate the desired amount of gold as exactly as possible. After Au deposition, the sample was post-annealed at 430 °C for 10 s and at 610 °C for 5 s resulting in the Si(5 5 3)-1 × 2-Au surface reconstruction which is shown in figure 1(a). Only for the H_2 exposure experiment, a slightly different preparation procedure (Au deposition at silicon wafer held at 600 °C) was applied which resulted in a slightly lower plasmonic resonance frequency (corresponding to longer plasmonic channels) in comparison with the other four experiments. Despite this slight difference in the plasmonic response, the RHEED analysis verified the reproducible preparation of the Si(5 5 3)-1 × 2-Au superstructure (figure 2) as a starting point for the different exposures and their resulting modifications.

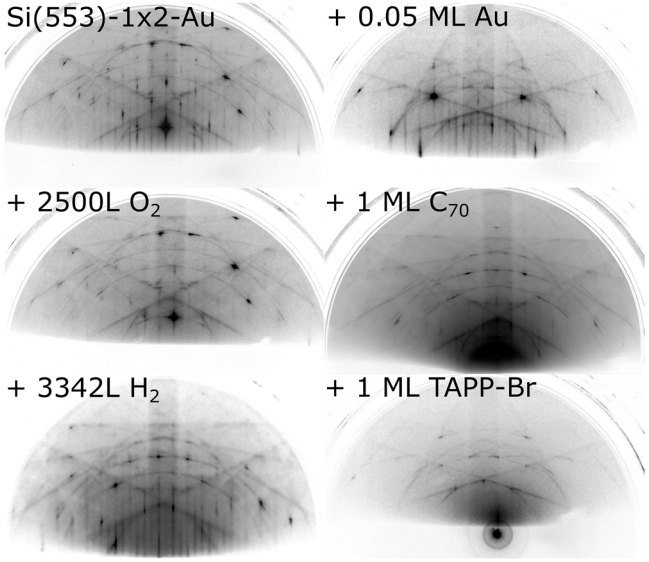

Figure 2. RHEED images at RT for the bare surface and for selected exposures (in Langmuir L) or coverages (in monolayers ML), respectively, as given. The superstructure features (dense vertical lines) are clearly visible for the bare surface gradually disappears for higher adsorbate coverage, which might have two reasons, the destroyed superstructure or the disordered adsorbate layer. The IR signal can clarify the situation further.

3.2. Adsorbates and exposure

IR spectra of the Si(5 5 3)-1 × 2-Au surface were studied for exposures to gaseous H_2 and O_2, respectively, at partial pressure in the 10^{-7} mbar range realized by backfilling the chamber through a leak valve. The spectra of the H_2-covered surfaces were recorded during exposure. In the figures we provide the H_2 exposures reached at the mid time of the IR measurement. For the O_2 exposure, the leak valve during the accumulation of IR spectra was closed which resulted in an immediate pressure drop by two orders of magnitude. The oxygen exposures given in the figures are those after each exposure step and before the IR measurement. RHEED analysis was performed directly after IR spectroscopy (see RHEED images for selected coverage in figure 2). The reversibility of the surface modification due to the H_2 exposure was proven by annealing the sample at 930 °C for 2 s and subsequent IR spectroscopy at RT.

C_{70} was thermally evaporated with a deposition rate of 0.0625 ML min^{-1} at a crucible temperature of 320 °C, never exceeding a pressure of 10^{-10} mbar up to a coverage of 2 ML according to the procedure reported in [27] (experiment A).

Besides the well-known C_{70}, and the gases H_2 and O_2, we selected the almost planar N-heteropolycyclic TAPP-Br (2,9-Bis- (heptafluoropropyl)-4,7,11,14-tetrabromo-1,3,8,10-tetraazaperopyrene-$C_{28}H_4Br_4F_{14}N_4$) molecule as an adsorbate to investigate the degrees of surface modification. Starting from 1,3,8,10-tetraazaperopyrenes, a multitude of compounds have been synthesized in recent years. Especially the core halogenation of those compounds provides great opportunities to systematically tune their molecular properties [43, 44] which are promising for the application as organic n-channel semiconductors. It has been previously established that TAPP-Br preferably lies flat on Au surfaces and is stable under ambient conditions [44]. Figure 1(b) shows the comparison of the molecular and the surface unit cell dimensions (according to [18]) and illustrates that for a flat adsorption geometry, a full monolayer corresponds to one molecule per surface unit cell.

TAPP-Br was thermally evaporated with a deposition rate of 0.1875 ML min^{-1} at a crucible temperature of 167 °C, never exceeding a pressure of $1.5 \cdot 10^{-10}$ mbar up to a coverage of 5 ML. A two-step doping experiment was performed by initial Au doping and subsequent deposition of TAPP-Br. The evaporation of additional Au atoms was carried out under similar conditions as in other studies ([25] up to 0.05 ML additional Au atoms deposited at RT), the following TAPP-Br deposition under the conditions as described above up to the coverage of 5 ML.

At this point, it is important to notice the different definitions of the monolayers for the various adsorbate species. For Au deposition (as doping of the superstructure), the definition of the monolayer as given above ($1\ ML_{Au} = 7.83 \cdot 10^{14}$ Au atoms/cm^2) applies, whereas the monolayer of C_{70} and TAPP-Br is defined here as the amount when each 1 × 2-Au unit cell is covered by one molecule as we illustrated in figure 1(b).

3.3. Infrared spectroscopy and data analysis

The infrared (IR) spectroscopic measurements were performed with a dry air purged Fourier transform IR (FTIR) spectrometer (Tensor 27, Bruker) using a broadband mercury cadmium telluride (MCT) detector. The FTIR spectrometer was directly connected to the UHV chamber via KBr windows. Only for the H_2 exposure experiment, a slightly different MCT detector (narrow band) was used. All measurements were performed with samples kept at RT. Reference spectra (flashed silicon wafer, spectra taken before the Au deposition) and the spectra after Au deposition, as well at the various exposure steps (H_2, O_2, Au, C_{70}, TAPP-Br, respectively) were scanned 200 times (within 86 s) at a resolution of 4 cm^{-1} (except for the H_2 exposure experiment for which the reference spectra were accumulated for 173 s). All measurements discussed in this paper were carried out in transmittance geometry under normal incidence of light. Due to the highly anisotropic character of the Si(5 5 3)-1 × 2-Au surface, the IR radiation was polarized either parallel (0°) or perpendicular (90°) to the Au chains. The relative transmittance spectra were obtained by dividing the spectra from samples with Au chains (and after the subsequent additional exposure, respectively) by the reference spectra for the Si surface before the gold deposition.

The relative transmittance spectra were analyzed within the theoretical framework previously reported in [25–27, 36]. Consequently, equation (4) was used as the fit model to analyze the experimental data and to extract the influence of the particular adsorbate on the plasmonic excitation of the gold-induced superstructure. The fit parameter $\Delta\omega$ describes the resonance broadening due to the distribution of lengths and is characteristic for a certain superstructure preparation. In case of C_{70} we have shown recently that there is no change in the chain length distribution during the adsorption of molecules [27] and the Gaussian broadening thus remains unchanged. However, this cannot be generally assumed and changes of the resonance position ω_{pl} indicate a changed average length (indicating a changed length distribution). In principle each data curve in one experimental set therefore has to be described by its individual Gaussian broadening parameter. However, if the electronic scattering ω_τ is much greater than $\Delta\omega$, the fitting procedure is no more sensitive to changes of the non-dominant parameter. As a useful approximation for our systems, we employed the same $\Delta\omega$ for all fits to spectra for the same initial superstructure preparation, including those with an eventually changing chain length distribution.

4. Results

4.1. Oxygen and hydrogen adsorption

The IR plasmonic signal (broad transmittance minimum in figure 3) of the Si(5 5 3)-Au surface indicates its strong 1D metallic character [25] which is reduced by hydrogen and by oxygen adsorption, respectively. The signal appears only for the incident electric field polarized along the Au chain

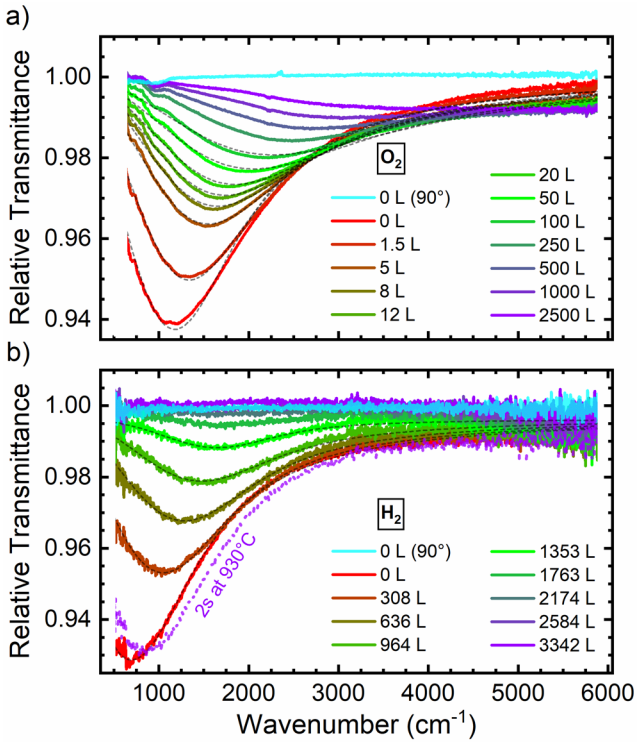

Figure 3. Relative transmittance spectra of the Si(5 5 3)-Au superstructure at RT for various exposures of O_2 (a) and H_2 (b) as given and polarization along the chain direction. Spectral fits according to equation (4) are indicated as dotted lines. For the polarization direction perpendicular to the chains (90°) no plasmonic signal is observed. In (b) the spectrum recorded after heating the H-covered sample at 930 °C is shown. It is almost equal to that of the unexposed superstructure.

direction. It is different for the two experiments because of the use and preparation of two different wafers. As apparent in figures 3(a) and (b), the peak area was reduced with increasing exposure. The disappearance of the plasmonic signal indicated the emergent insulating character of the surface. For hydrogen adsorption the process could be reversed by heating to 930 °C in UHV. The position of the transmittance minimum shifted to higher frequencies upon increasing exposure, which together with the decreasing peak area implied a shortening of the average length of the conducting channels. For hydrogen adsorption, the developing insulating phase may be explained by the electron transfer from the H adsorbates [23, 24]. The adsorption process starts with H bonding to the step edges Si atoms. The IR spectra reveal an ongoing process towards the insulating state whereas a theoretical treatment reported in the literature [23] predicted a return of the conducting phase at higher H coverage. It is interesting to see the RHEED pattern of the superstructure still existing at the highest exposure (figure 2). The insulating behavior is therefore mainly the result of doping, which is consistent with the return of the metallic phase simply by removing the hydrogen. For oxygen the insulating character was also found to increase with exposure, in accordance with other experiments that previously revealed only a small decrease in the dc surface conductivity upon a 30 L oxygen exposure [22]. For our oxygen-exposure experiments the final coverage did not correspond to the

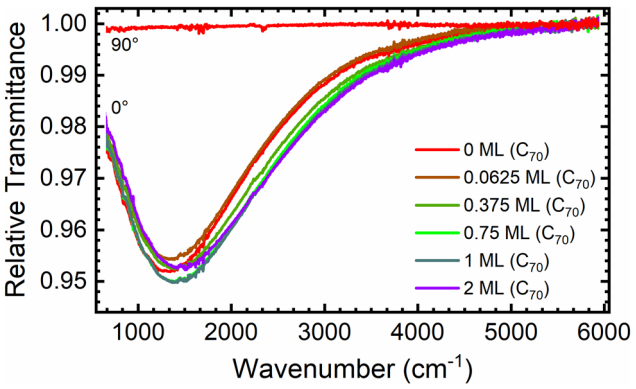

Figure 4. Relative transmittance spectra of the Si(5 5 3)-Au superstructure at RT for various C_{70} coverage. As in figure 3, the results for the two polarization directions are shown for the pristine superstructure.

saturation of the process. Notably, at that final coverage the very broad spectral feature towards higher wavenumbers indicated a stronger IR absorption compared with the reference spectrum, which might be due to interband transitions of the oxidized surface. In the RHEED pattern, the superstructure could still be recognized even for the final coverage, while the reflections were much more blurred if compared with the data obtained upon the final H_2 coverage.

4.2. C_{70} adsorption

A fullerene was chosen first for molecular adsorption studies because of the chemical stability that let us expect that the molecules do not destroy the surface structure. C_{70} instead of C_{60} was used because of its higher IR activity of vibrational modes [45]. The changes of the IR plasmonic spectrum with C_{70} exposure appear marginal if compared with the changes upon hydrogen and oxygen exposure. The most striking result has been the complete persistence of the plasmonic feature (figure 4). As already reported [27], the signal can be measured with the same size up to C_{70} thicknesses of more than 20 nm. Careful data analysis yielded a very small increase of the signal intensity (due to electron uptake by C_{70}) and of the resonance position within the first ML of C_{70} ([27] and see below). It therefore appears that with C_{70} (and possibly also with C_{60}) the conducting channels of the superstructure are stabilized and almost unaffected. A detailed analysis of the RHEED pattern for 1 ML C_{70} in figure 2 was precluded by a partially blurred pattern that might be due to a disorder of the adsorbate layer. In figure 4, vibrational excitations are not visible because their signal size is at the noise level of these experiments. Results for thicker C_{70} layers [27] make obvious that plasmonic enhancement (surface enhanced IR absorption, SEIRA) does not occur, as expected for the ultrathin 1D metallic chains [33].

4.3. TAPP-Br adsorption

A completely different behavior has been observed for TAPP-Br adsorption. The relevant electronic energy levels (ionization energy, electron affinity) [43, 44] are about 1 eV

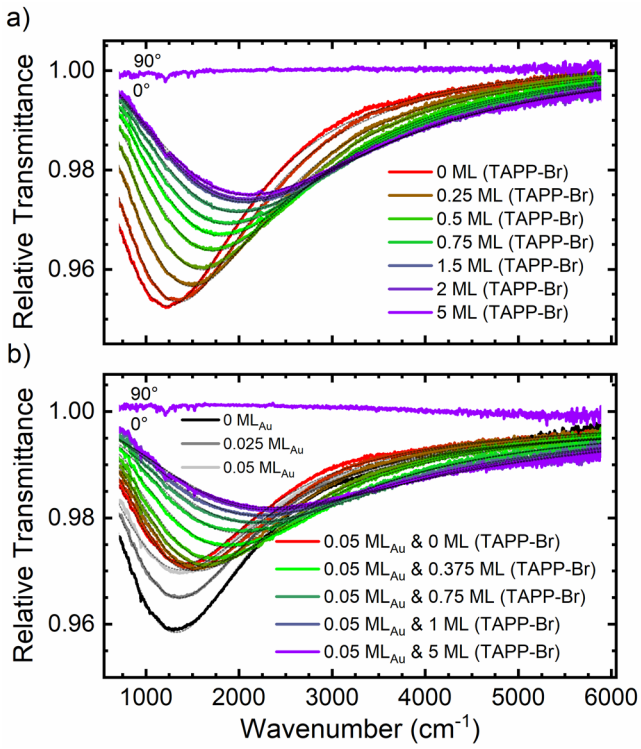

Figure 5. Relative transmittance spectra of the Si(5 5 3)-Au superstructure at RT for various coverage with TAPP-Br (a) and with TAPP-Br after the RT deposition of 0.05 ML Au on that superstructure (b). Spectral fits according to equation (4) are indicated as dotted lines. As in the spectra shown above, polarization is along the chains (0°) or perpendicular to them (90°), respectively.

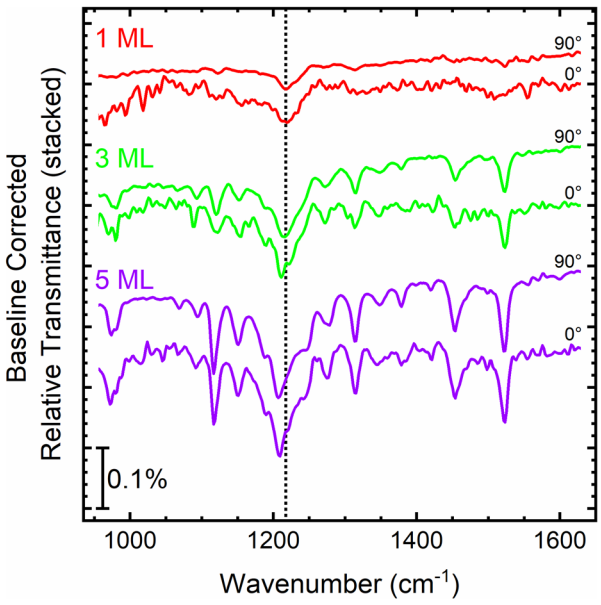

Figure 6. Baseline corrected relative transmittance spectra of the TAPP-Br covered Si(5 5 3)-Au superstructure at RT for three different coverages as given. The vertical line marks the strong IR band of the CF_3 stretching vibrations in the molecular plane. Its appearance in the first monolayer indicates adsorption with the molecular plane parallel to the surface. However, compared to thicker layers, the band is at higher values for the first ML, which might be related to a molecular deformation as studied in [44] for adsorption on Au(1 1 1). The spectra for the polarization perpendicular to the chains (90°) were acquired with 33 000 scans.

higher than those of C_{70} [46] but still separated from the Fermi level of the gold surface and probably of the superstructure. It is thus not surprising that the plasmonic signal was not destroyed by the adsorption of TAPP-Br, see figure 5(a). However, we observed a shift of the resonance to higher frequencies as well as a strong broadening. At about 1 ML TAPP-Br, these changes reached saturation, while the remaining plasmonic resonances were heavily damped. The spectra obtained upon baseline correction and the amplified depiction of the vibrational bands of the molecule (figure 6) were consistent with the presence of the molecules on the surface. Moreover, a change of the vibrational bands with coverage indicated a change in molecular orientation of the attached $(CF_2)_2CF_3$ groups in the molecular layers away from the surface, as previously noted for TAPP-Br on gold [44]. It should be noticed that the IR activity of the vibrations of TAPP-Br is much higher than that of C_{70} and thus signals could be observed in our experiments already at a very low coverage. Vibrational spectra for polarization perpendicular to the chains were taken with a much higher accumulation time and thus appear less noisy in figure 6. There are no deviations in IR spectra for the two polarization directions obvious, which indicates the absence of plasmonic enhancement, as seen for C_{70} [27]. Also, conclusions on anisotropic adsorption in the surface plane cannot be drawn. Closer inspection of the RHEED pattern in figure 2 revealed that it is nearly impossible to see the superstructure features, most probably because of disorder in the molecular layer. A conclusion with regard to the presence of the plasmonic channels was thus only possible by IR spectroscopy.

4.4. Gold and TAPP-Br adsorption

A surprisingly different behavior upon TAPP-Br adsorption was found, if the superstructure was doped with 0.05 ML Au atoms, which is shown in figure 5(b). It is well known that the additional gold atoms donate electrons to the surface states and lead to a lower 1D plasma frequency parameter [25] and a higher Fermi energy [47]. With a higher Fermi energy, a better overlap with the LUMO of the TAPP-Br supports electron transfer to the TAPP-Br adsorbates. In this way the increase of the peak area with the subsequent TAPP-Br coverage up to 1 ML can be accounted for. While this increase cannot be seen readily in figure 5(b) because of line broadening, the spectral analysis based on equation (4) provides clarity.

5. Discussion

In figure 7 the parameters obtained for the best spectral fits with equation (4) are compared based on normalized data. The normalization values used for the electronic scattering rate, the plasmonic resonance frequency, and the Gaussian broadening are given in table 1. For this analysis the precise control of the stability of the IR background (of the 100%-line over the relevant range) was crucial. Therefore, the experiments have

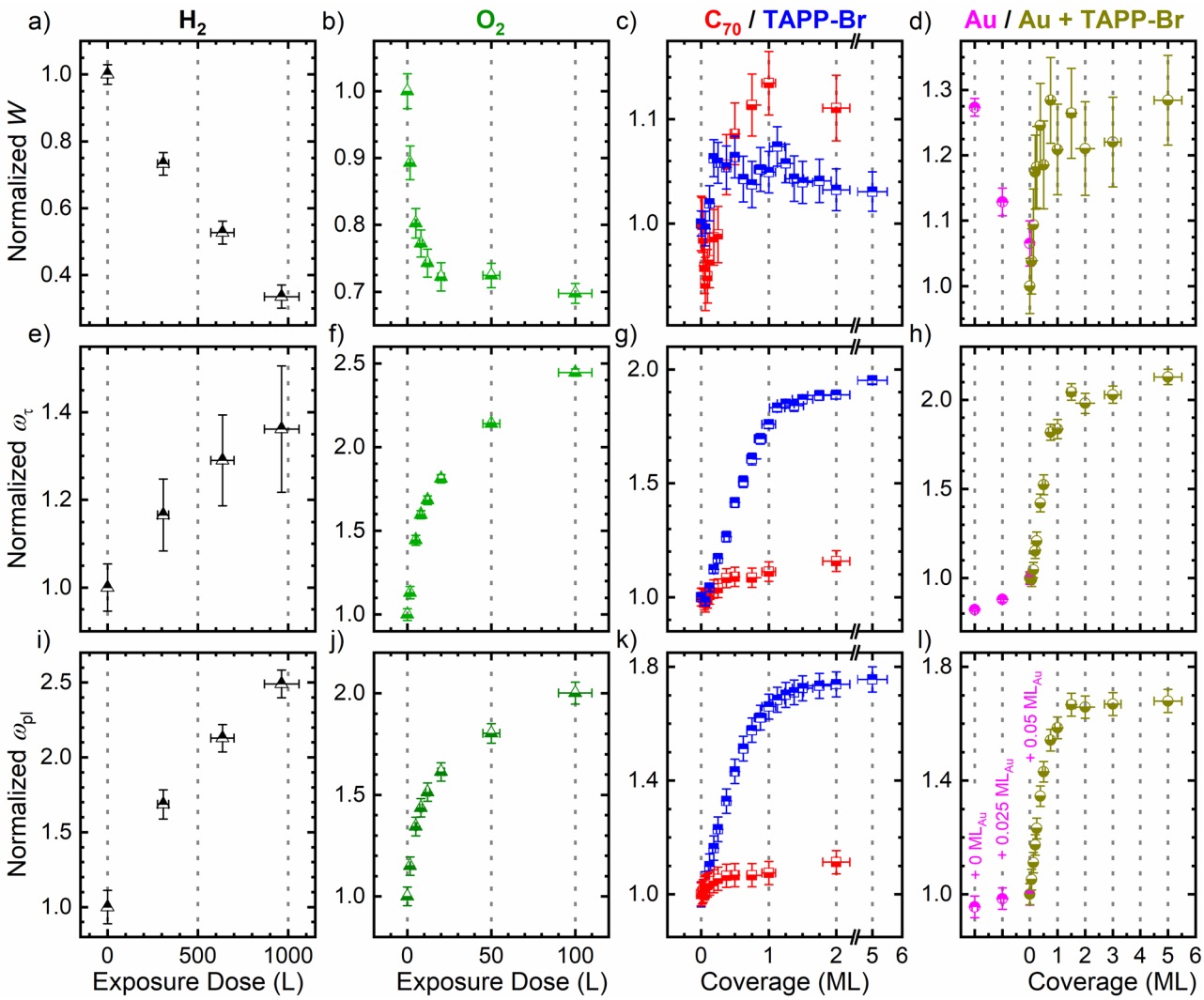

Figure 7. Comparison of the fit parameters versus increasing exposure and coverage. To provide better comparison, the results are displayed after a normalization to the value for zero adsorbate coverage. The values used for the normalization of the electronic scattering rate and the plasmonic resonance frequency, as well as the results for the Gaussian broadening are given in table 1.

been performed with special care with regard to the stability of the detector and the interferometer. In all fits the plasmonic frequeny ω_{pl} and the electronic scattering rate ω_τ turned out to be very robust parameters, i.e. their values barely depended on any background instabilities.

On the other hand, for the parameter $W = \frac{N}{A}\frac{n_{1D}le^2}{\varepsilon_0 m^* c}$ background instabilities produce larger errors. Different trends of W with coverage below 0.1 ML are related to defect sites, such as chain ends [27].

For oxygen adsorption, the data for increasing exposure seem to indicate saturation, while the partial oxygen pressure was always in the UHV range and further oxidation proceeded slowly. We note that oxidation usually strongly depends on pressure and proceeds much faster at partial pressures above the UHV range.

For the parameter W representing the spectral weight of the plasmonic excitation, similar tendencies are obvious for H_2 and O_2 exposure on the one side and for TAPP-Br and C_{70} coverage on the other. For the first two gases, the decay of the spectral weight W reflects the transition to the insulating phase. On the other side, the only small changes resulting from the adsorption of the two organic molecules indicate that charge transfer is extremely small, albeit somewhat greater for TAPP-Br on the gold-doped surface where the intial W of the pristine superstructure is reached at about 1 ML. This experiment shows that it is possible to control the conductivity of the plasmonic channels by an appropriate choice of the adsorbate [24]. Within our experimental accuracy, a clear change of the spectral weight is not seen for coverage above 1 ML TAPP-Br or C_{70}, respectively. Both the molecules seem to protect the gold superstructure and its metallic state. However, the electrical conductivity also depends on electronic scattering.

Electronic scattering increases for all adsorbates. For C_{70} it is quite small as to be expected for surface friction [27] while it is much larger for the chains that develop towards the insulating phase under H_2 and O_2 adsorption. However, it is surprisingly large for TAPP-Br where charge transfer is not significant, which might indicate a crucial role of the heavy Br atoms in this molecule. Such heavy atoms lead to low-energy vibrations of the molecule which are excited already at room

Table 1. Values for the electronic scattering rate ω_τ and the plasmonic resonance frequency ω_{pl} which are used to normalize the data in figure 7, as well as the results for the Gaussian broadening $\Delta\omega$. For the gas exposure experiments, the values for a coverage of 0 L are given. The values for 0 ML coverage are given for all others.

	H_2	O_2	C_{70}	TAPP-Br	Au	Au + TAPP-Br
ω_τ (cm^{-1})	1087 ± 59	1351 ± 47	1349 ± 53	1575 ± 15	1532 ± 12	1796 ± 53
ω_{pl} (cm^{-1})	560 ± 62	1116 ± 51	1261 ± 51	1169 ± 51	1283 ± 51	1395 ± 52
$\Delta\omega$ (cm^{-1})	357 ± 37	259 ± 13	423 ± 18	277 ± 5	202 ± 8	131 ± 26

temperature and so might contribute to electronic damping. The flat molecular orientation on the surface will also be significant for electronic damping and, in addition, induce the strong shift of the resonance position.

The persistance of the full spectral weight contradicts any shortening of conducting channels and indicates two possible factors for the explanation of the resonance shift. One is the refractice index embedding the channels which cannot be smaller with molecules than without them, which is why this effect can be ruled out. On the other hand, the confinement parameter b could play a key role as its decrease would lead to an increase in the plasmonic frequencies according to $\sqrt{\ln(l/b\pi)}$. In particular, since the plasmonic resonance frequency increases, the 1D confinement of the conducting channel should be increased by the adsorption of TAPP-Br molecules. Both, the resonance frequency shift and the increase of electronic scattering saturate at about 1 ML TAPP-Br, in accordance with the observation for the spectral weight.

6. Conclusions

Our IR studies have provided new insights into adsorbate-surface interactions as reflected in the plasmonic signals of the quasi-1D conducting channels of the Si(5 5 3)-Au surface superstructure. We have shown and discussed different cases of adsorbate induced changes of the plasmonic resonance. With hydrogen and oxygen adsorption the gradual transition to the insulating surface is observed in the decrease of the peak area. RHEED images and the inspection of the reversibility of the plasmonic signal upon desorption have indicated whether the structure was destroyed or the transition was mainly due to doping into the conducting channels. With the fullerene C_{70}, the plasmonic spectrum persisted in all features even under conditions of multilayer coverage. For the N-heteropolycyclic aromatic TAPP-Br molecules another type of behavior was observed. These molecules in the first monolayer strengthen the 1D character of the conducting channels while giving rise to an increased electronic damping. Both effects indicate the important role of the spill-out of the electronic wave function at surfaces on the transport properties of interfaces. This has previously been referred to as the push-back [48] or pillow [49] (cushion [50]) effect, respectively, which describes the changes in the work function of surfaces due to physisorbed molecules in terms of the compression of the surface wave function by the adsorbates. Our observation might serve as another experimental manifestation of that effect. We have also shown that weak Au-doping of the surface modifies the adsorbate induced effects and gives rise to charge transfer, so that the plasmonic signal of the 1D channels is raised again to the value of the pristine surface.

Acknowledgments

The work was financially supported by the German Science Foundation (DFG) via the collaborative research center SFB 1249 and via the reasearch unit FOR 1700. MT acknowledges support from the Heidelberg Graduate School for Fundamental Physics (HGSFP).

ORCID iDs

Annemarie Pucci https://orcid.org/0000-0002-9038-4110

References

[1] Yeom H W *et al* 1999 Instability and charge density wave of metallic quantum chains on a silicon surface *Phys. Rev. Lett.* **82** 4898–901
[2] Crain J N, McChesney J L, Zheng F, Gallagher M C, Snijders P C, Bissen M, Gundelach C, Erwin S C and Himpsel F J 2004 Chains of gold atoms with tailored electronic states *Phys. Rev.* B **69** 125401
[3] Crain J N and Himpsel F J 2006 Low-dimensional electronic states at silicon surfaces *Appl. Phys.* A **82** 431–8
[4] Snijders P C and Weitering H H 2010 Colloquium: electronic instabilities in self-assembled atom wires *Rev. Mod. Phys.* **82** 307–29
[5] Hasegawa S 2010 Quasi-one-dimensional metals on semiconductor surfaces with defects *J. Phys.: Condens. Matter* **22** 084026
[6] Gurlu O, Adam O A O, Zandvliet H J W and Poelsema B 2003 Self-organized, one-dimensional Pt nanowires on Ge(0 0 1) *Appl. Phys. Lett.* **83** 4610–2
[7] Schäfer J, Schrupp D, Preisinger M and Claessen R 2006 Conduction states with vanishing dimerization in Pt nanowires on Ge(0 0 1) observed with scanning tunneling microscopy *Phys. Rev.* B **74** 041404(R)
[8] Blumenstein C, Meyer S, Mietke S, Schäfer J, Bostwick A, Rotenberg E, Matzdorf R and Claessen R 2013 Au-induced quantum chains on Ge(0 0 1)—symmetries, long-range order and the conduction path *J. Phys.: Condens. Matter* **25** 014015
[9] Choi W H, Kang P G, Ryang K D and Yeom H W 2008 Band-structure engineering of gold atomic wires on silicon by controlled doping *Phys. Rev. Lett.* **100** 126801
[10] Chung H V V, Kubber C J, Han G, Rigamonti S, Sanchez-Portal D, Enders D, Pucci A and Nagao T 2010 Optical detection of plasmonic and interband excitations in 1-nm-wide indium atomic wires *Appl. Phys. Lett.* **96** 243101
[11] Erwin S C and Himpsel F J 2010 Intrinsic magnetism at silicon surfaces *Nat. Commun.* **1** 1–6

[12] Biedermann K, Regensburger S, Fauster T, Himpsel F J and Erwin S C 2012 Spin-split silicon states at step edges of Si(5 5 3)-Au *Phys. Rev.* B **85** 245413
[13] Barke I, Zheng F, Bockenhauer S, Sell K, von Oeynhausen V, Meiwes-Broer K H, Erwin S C and Himpsel F J 2009 Coverage-dependent faceting of Au chains on Si(5 5 7) *Phys. Rev.* B **79** 155301
[14] Ghose S K, Robinson I K, Bennett P A and Himpsel F J 2005 Structure of double row quantum wires in Au/Si(5 5 3) *Surf. Sci.* **581** 199–206
[15] Voegeli W, Takayama T, Shirasawa T, Abe M, Kubo K, Takahashi T, Akimoto K and Sugiyama H 2010 Structure of the quasi-one-dimensional Si(5 5 3)-Au surface: gold dimer row and silicon honeycomb chain *Phys. Rev.* B **82** 075426
[16] Krawiec M 2010 Structural model of the Au-induced Si(5 5 3) surface: double Au rows *Phys. Rev.* B **81** 115436
[17] Aulbach J, Schäfer J, Erwin S C, Meyer S, Loho C, Settelein J and Claessen R 2013 Evidence for long-range spin order instead of a peierls transition in Si(5 5 3)-Au chains *Phys. Rev. Lett.* **111** 137203
[18] Hafke B, Frigge T, Witte T, Krenzer B, Aulbach J, Schäfer J, Claessen R, Erwin S C and Horn-Von Hoegen M 2016 Two-dimensional interaction of spin chains in the Si(5 5 3)-Au nanowire system *Phys. Rev.* B **94** 161403
[19] Lichtenstein T, Tegenkamp C and Pfnür H 2016 Lateral electronic screening in quasi-one-dimensional plasmons *J. Phys.: Condens. Matter* **28** 354001
[20] Lichtenstein T, Mamiyev Z, Braun C, Sanna S, Schmidt W G, Tegenkamp C and Pfnür H 2018 Probing quasi-one-dimensional band structures by plasmon spectroscopy *Phys. Rev.* B **97** 165421
[21] Mamiyev Z, Lichtenstein T, Tegenkamp C, Braun C, Schmidt W G, Sanna S and Pfnür H 2018 Plasmon spectroscopy: robust metallicity of Au wires on Si(5 5 7) upon oxidation *Phys. Rev. Mater.* **2** 066002
[22] Edler F, Miccoli I, Stöckmann J P, Pfnür H, Braun C, Neufeld S, Sanna S, Schmidt W G and Tegenkamp C 2017 Tuning the conductivity along atomic chains by selective chemisorption *Phys. Rev.* B **95** 125409
[23] Hogan C, Speiser E, Chandola S, Suchkova S, Aulbach J, Schäfer J, Meyer S, Claessen R and Esser N 2018 Controlling the local electronic properties of Si(5 5 3)-Au through hydrogen doping *Phys. Rev. Lett.* **120** 166801
[24] Suchkova S, Hogan C, Bechstedt F, Speiser E and Esser N 2018 Selective adsorption of toluene-3,4-dithiol on Si(5 5 3)-Au surfaces *Phys. Rev.* B **97** 045417
[25] Hötzel F, Galden N, Baur S and Pucci A 2017 One-dimensional plasmonic excitations in gold-induced superstructures on Si(5 5 3): impact of gold coverage and silicon step edge polarization *J. Phys. Chem.* C **121** 8120–7
[26] Hötzel F, Seino K, Chandola S, Speiser E, Esser N, Bechstedt F and Pucci A 2015 Metal-to-insulator transition in Au chains on Si(111)-5 × 2-Au by band filling: infrared plasmonic signal and *ab initio* band structure calculation *J. Phys. Chem. Lett.* **6** 3615–20
[27] Tzschoppe M, Huck C, Hötzel F and Pucci A 2018 C_{70} increases the plasmonic signal of gold-atom chains on Si(5 5 3) *Surf. Sci.* **678** 32–7
[28] Crain J, Stiles M, Stroscio J and Pierce D 2006 Electronic effects in the length distribution of atom chains *Phys. Rev. Lett.* **96** 156801
[29] Aizpurua J, Bryant G W, Richter L J, García de Abajo F J, Kelley B K and Mallouk T 2005 Optical properties of coupled metallic nanorods for field-enhanced spectroscopy *Phys. Rev.* B **71** 235420
[30] Bernadotte S, Evers F and Jacob C R 2013 Plasmons in molecules *J. Phys. Chem.* C **117** 1863–78
[31] Moudgil R K, Garg V and Pathak K N 2010 Confinement and correlation effects on plasmons in an atom-scale metallic wire *J. Phys.: Condens. Matter* **22** 135003
[32] Schulz H J 1993 Wigner crystal in one dimension *Phys. Rev. Lett.* **71** 1864–7
[33] Neuman T, Huck C, Vogt J, Neubrech F, Hillenbrand R, Aizpurua J and Pucci A 2015 Importance of plasmonic scattering for an optimal enhancement of vibrational absorption in SEIRA with linear metallic antennas *J. Phys. Chem.* C **119** 26652–62
[34] Vogt J, Hoang C V, Huck C, Neubrech F and Pucci A 2016 How intrinsic phonons manifest in infrared plasmonic resonances of crystalline lead nanowires *J. Phys. Chem.* C **120** 19302–7
[35] Teschner U and Hübner K 1990 IR-spectroscopic data of thin insulating films on semiconductors. New methods of interpretation and analysis *Phys. Status Solidi* **159** 917–26
[36] Hötzel F, Seino K, Huck C, Skibbe O, Bechstedt F and Pucci A 2015 Metallic properties of the Si(1 1 1)—5 × 2—Au surface from infrared plasmon polaritons and *ab initio* theory *Nano Lett.* **15** 4155–60
[37] Fahsold G, Sinther M, Priebe A, Diez S and Pucci A 2002 Adsorbate-induced changes in the broadband infrared transmission of ultrathin metal films *Phys. Rev.* B **65** 235408
[38] Pischel J, Skibbe O and Pucci A 2012 Anisotropic resistance of the clean and oxygen-covered Cu(1 1 0) surface in the infrared *J. Phys. Chem.* C **116** 14014–21
[39] Persson B N J 1992 Adsorbate-induced surface resistivity and nonlocal optics *Chem. Phys. Lett.* **197** 7–11
[40] Tobin R G 2002 Mechanisms of adsorbate-induced surface resistivity—experimental and theoretical developments *Surf. Sci.* **502–3** 374–87
[41] Dumas P, Hein M, Otto A, Persson B N J, Rudolf P, Raval R and Williams G P 1999 Friction of molecules at metallic surfaces: experimental approach using synchrotron infrared spectroscopy *Surf. Sci.* **433–5** 797–805
[42] Hein M, Dumas P, Otto A and Williams G P 1999 Friction of conduction electrons with adsorbates: simultaneous changes of DC resistance and broadband IR reflectance of thin Cu(1 1 1) films exposed to CO *Surf. Sci.* **419** 308–20
[43] Geib S, Zschieschang U, Gsänger M, Stolte M, Würthner F, Wadepohl H, Klauk H and Gade L H 2013 Core-brominated tetraazaperopyrenes as n-channel semiconductors for organic complementary circuits on flexible substrates *Adv. Funct. Mater.* **23** 3866–74
[44] Hahn L, Maaß F, Bleith T, Zschieschang U, Wadepohl H, Klauk H, Tegeder P and Gade L H 2015 Core halogenation as a construction principle in tuning the material properties of tetraazaperopyrenes *Chem. Eur. J.* **21** 17691–700
[45] Chase B, Herron N and Holler E 1992 Vibrational spectroscopy of fullerenes (C_{60} and C_{70}). Temperature dependant studies *J. Phys. Chem.* **96** 4262–6
[46] Echegoyen L and Echegoyen L E 1998 Electrochemistry of fullerenes and their derivatives *Acc. Chem. Res.* **31** 593–601
[47] Song I, Oh D, Shin H, Ahn S-J, Moon Y, Woo S, Choi H J, Park C-Y and Ahn J R 2015 Direct momentum-resolved observation of one-dimensional confinement of externally doped electrons within a single subnanometer-scale wire *Nano Lett.* **15** 281–8
[48] Ishii H, Sugiyama K, Ito E and Seki K 1999 Energy level alignment and interfacial electronic structures at organic/metal and organic/organic interfaces *Adv. Mater.* **11** 605–25
[49] Vázquez H, Dappe Y J, Ortega J and Flores F 2007 Energy level alignment at metal/organic semiconductor interfaces: 'pillow' effect, induced density of interface states, and charge neutrality level *J. Chem. Phys.* **126** 144703
[50] Witte G, Lukas S, Bagus P S and Wöll C 2005 Vacuum level alignment at organic/metal junctions: 'cushion' effect and the interface dipole *Appl. Phys. Lett.* **87** 263502